Calculating Non-Potentialilty in Solar Active Regions Using SDO/HMI Vector Magnetic Field Data

M. G. Bobra[1], J. T. Hoeksema[1]

[1]*Stanford University*

Abstract: Non-potential magnetic fields in solar active regions are thought to be associated with flare occurrence. In this study, we parametrize the non-potentiality of several active regions, using data from the Helioseismic and Magnetic Imager (HMI) aboard the Solar Dynamics Observatory (SDO), and correlate these parameters with flare occurrence.

In particular, we focus on a parameter that we call the Gradient-Weighted Inversion Line Length (GWILL). Using data from SOHO/MDI, Mason and Hoeksema (2010) found that GWILL generally tends to increase before a solar flare. We investigate whether extending the analysis of Mason et. al. to a three-dimensional field enables us to derive better near real-time indicators of flare occurrence.

Before HMI, the availability of vector magnetograms was sparse at best. HMI provides continuous vector magnetogram data at a 12-minute cadence. As such, this study represents the first parametrization of non-potentiality in solar active regions using continuous vector magnetic field data.

Introduction□□

This study is one in a long line of work ultimately designed to predict solar activity, but immediately designed to test the validity of the vector magnetogram data from SDO. It is believed that parameterizations of the photospheric magnetic field can be correlated with solar activity. The HMI team will be producing these parameters in near real-time to aid those interested in predicting solar activity. Section 1 describes the process of creating vector magnetogram data. Section 2 shows spaceweather parameters as a function of time for two active regions. Section 3 highlights a particular parameter. Section 4 describes our conclusions.

Section 1: Creating Vector Magnetograms

This study used 720-second cadence, Lambert azimuthal equal area projected, fully disambiguated vector magnetogram data from SDO/HMI. Below is a schematic representation of how these data are created.

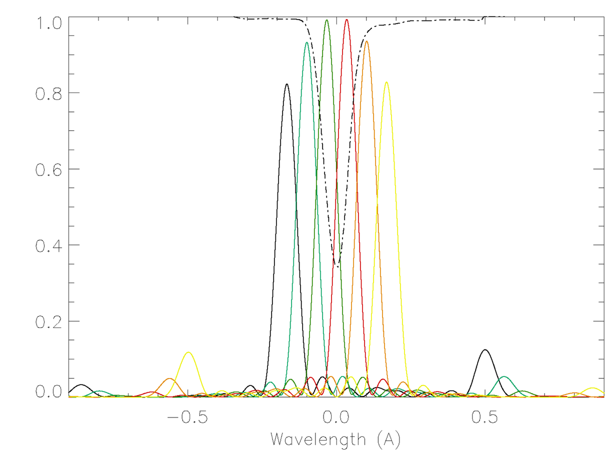

Step 1: In one 720-second interval, HMI samples 6 points across the baseline spectral line of 6173.3 Å, measures 6 polarization states (I, Q, U, V, LCP (I-V), and RCP (I+V)) per line, and takes 6 filtergrams per polarization state, for a total of 216 filtergrams.

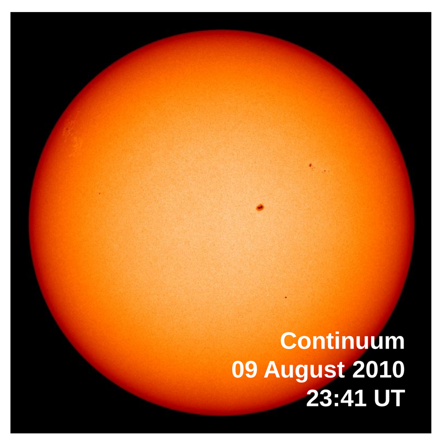

Step 2: The 6 filtergrams per unique combination of polarization state and wavelength are corrected for solar rotation and then temporally averaged to a target (or observation) time, for a total of 36 intermediate products.

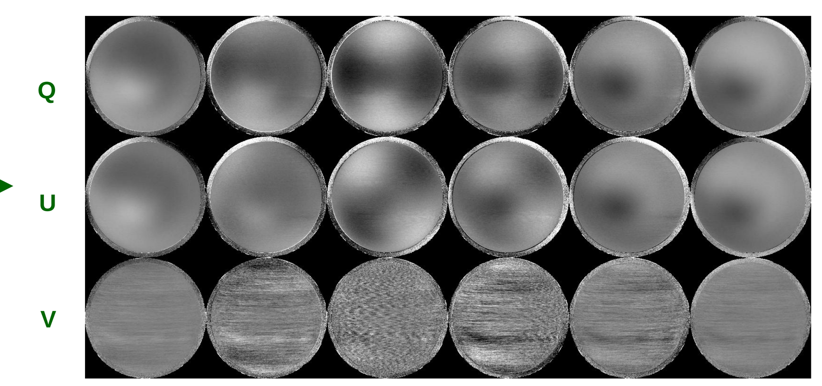

Step 3: A polarization calibration is applied to reduce the 36 intermediate data products into the four Stokes polarization states (I, Q, U, and V) per wavelength, for a total of 24 final level 1.5 data products (Schou et al., 2010).

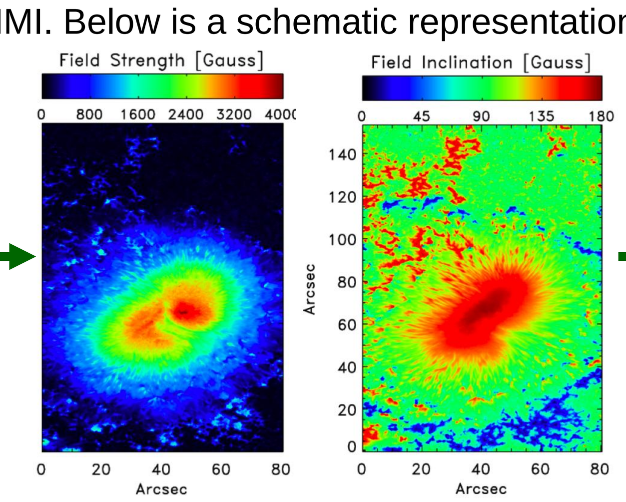

Step 5: These 24 I, Q, U, and V data are inverted using the Very Fast Inversion of the Stokes Vector (VFISV) inversion code, which assumes a Milne-Eddington model of the solar atmosphere, to yield the vector magnetogram data (Borrero et al, 2010).

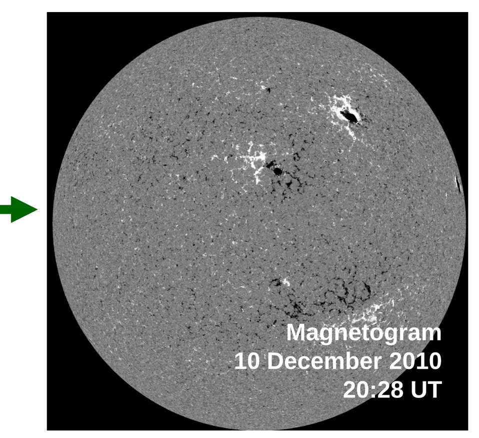

Step 6: Using a minimum energy method to resolve the 180º ambiguity, the inverted vector data is disambiguated to yield the magnetic field components in Cartesian coordinates: Bx, By, and Bz (Metcalf, 1994; Leka, K.D. et al. 2009). The data arrays containing each of these components are then reprojected using the Lambert azimuthal equal area projection.

Section 2: Spaceweather Parameters

Fourteen spaceweather parameters, outlined in Leka and Barnes (2003), were computed using the disambiguated vector magnetogram data. These plots show the evolution of said parameters as a function of time for two active regions: (1) AR 1117, a nonflaring region, from July 1, 2010 at 12:00 UT to July 4, 2010 at 00:00 UT, and (2) AR 1084, from October 25, 2010 at 00:00 UT to October 26, 2010 at 06:00 UT, which produced a C2-class flare; the peak of the GOES X-Ray Flux for this event was at 22:10 UT on October 25 -- on the plots below, that is 22 hours from the start of relative time.

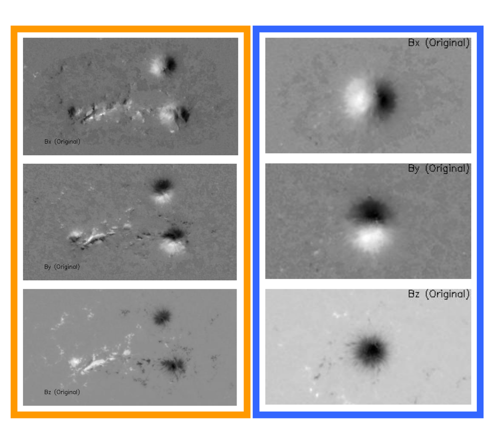

Total Unsigned Flux

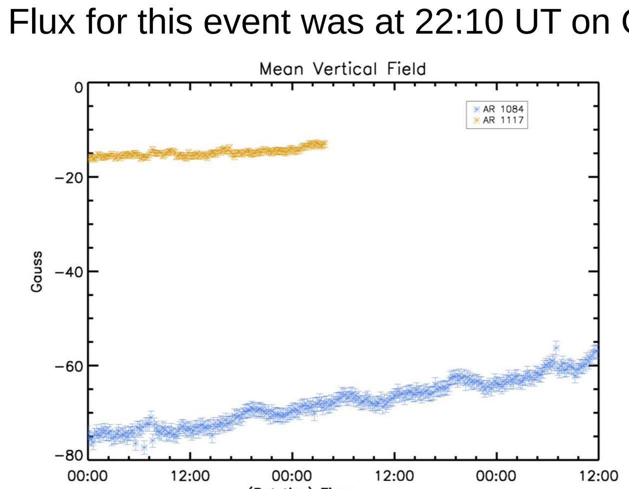

$B_z = \boldsymbol{B} \cdot \boldsymbol{e}_z$

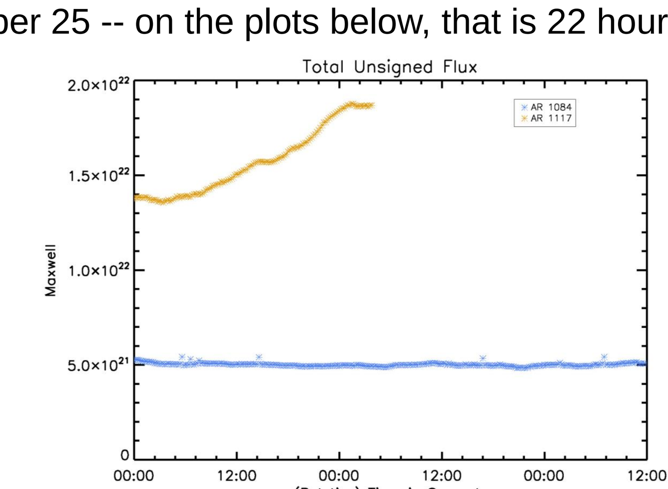

$\Phi_{\rm tot} = \sum |B_z|\, dA$

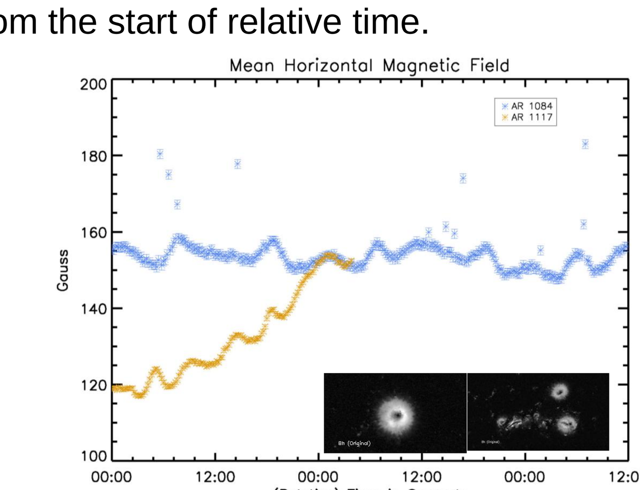

$B_h = \sqrt{B_x^2 + B_y^2}$

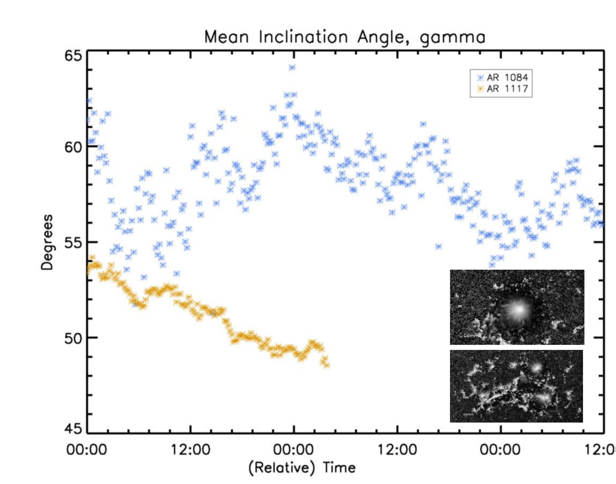

$\gamma = \tan^{-1}(B_z/B_h)$

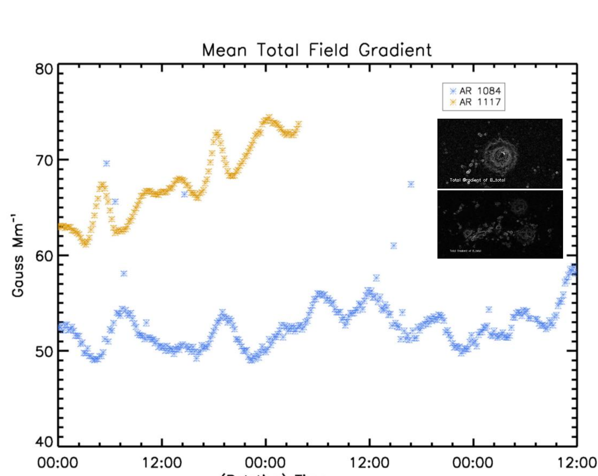

$|\nabla_h B| = \sqrt{(\partial B/\partial x)^2 + (\partial B/\partial y)^2}$

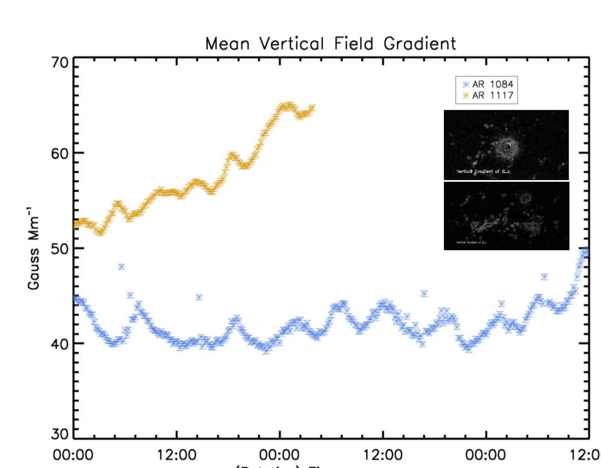

$|\nabla_h B_z| = \sqrt{(\partial B_z/\partial x)^2 + (\partial B_z/\partial y)^2}$

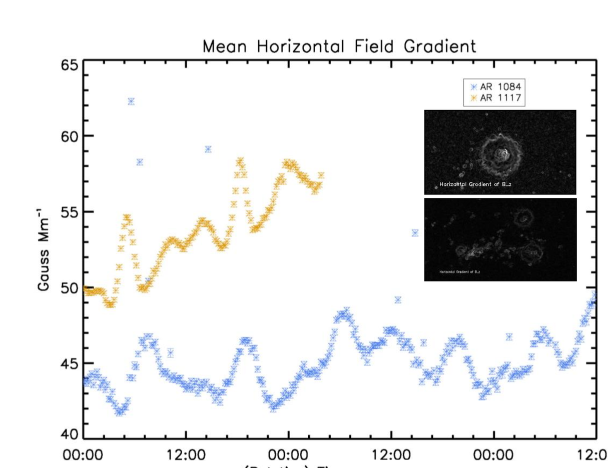

$|\nabla_h B_h| = \sqrt{(\partial B_h/\partial x)^2 + (\partial B_h/\partial y)^2}$

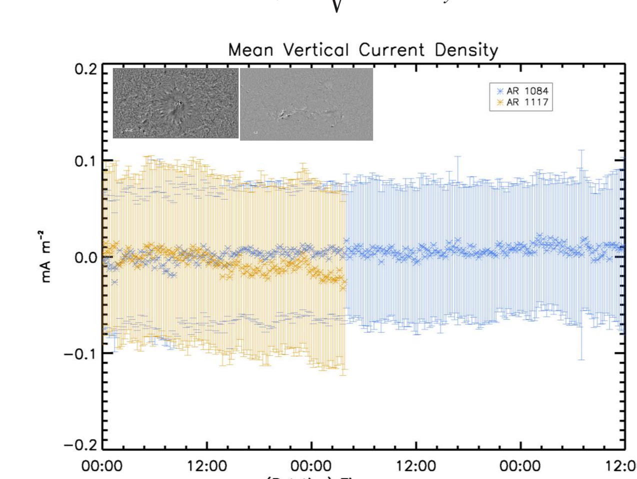

$J_z = (\partial B_y/\partial x - \partial B_x/\partial y)/\mu_0$

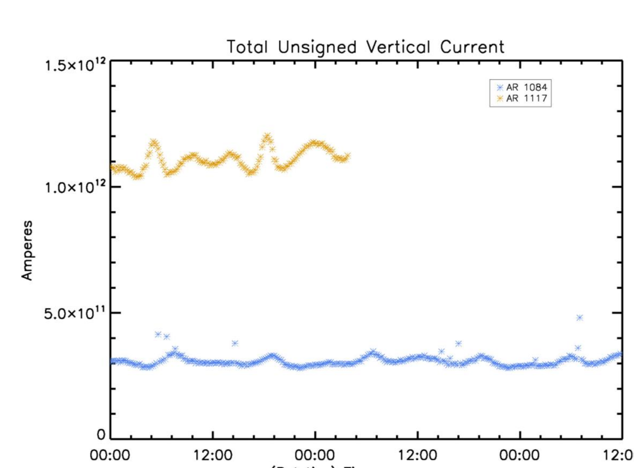

$I_{\rm tot} = \sum |J_z|\, dA$

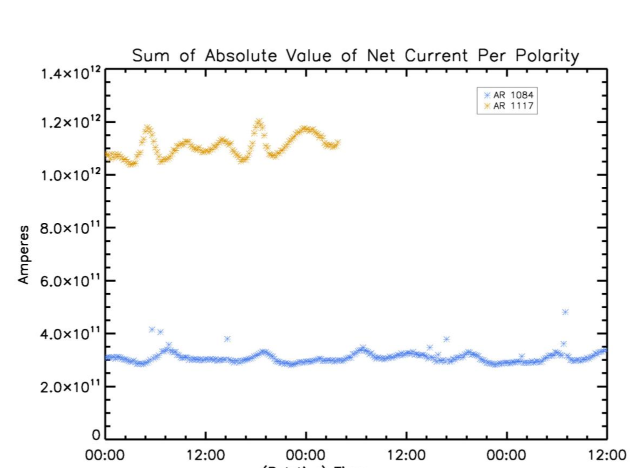

$|I_{\rm net}^B| = |\sum J_z(B_z > 0)\, dA| + |\sum J_z(B_z < 0)\, dA|$

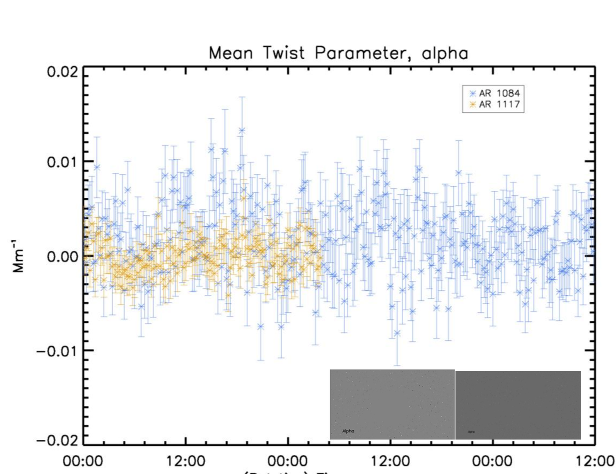

$\alpha = CJ_z/B_z$

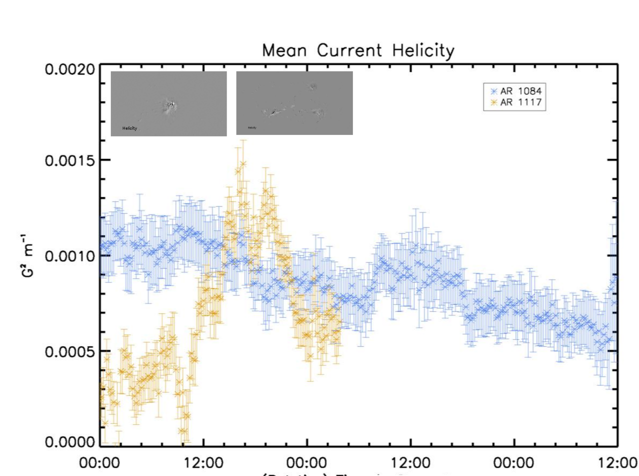

$h_c = CB_z(\partial B_y/\partial x - \partial B_x/\partial y)$

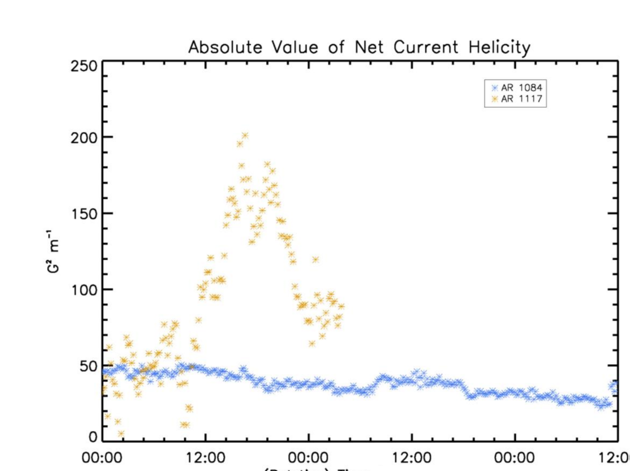

$|H_c^{\rm net}| = |\sum h_c\, dA|$

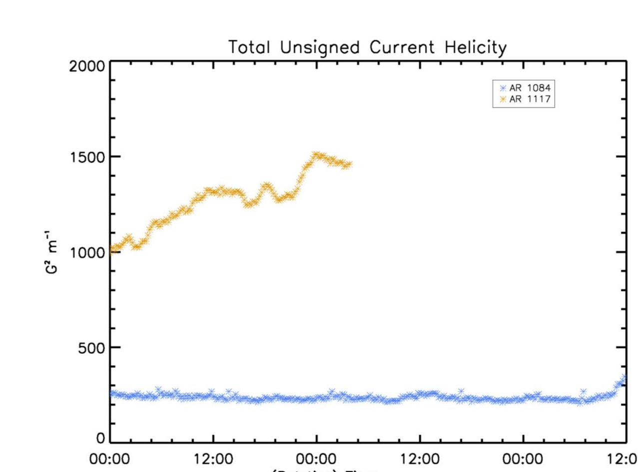

$H_c^{\rm tot} = \sum |h_c|\, dA$

Section 3: Gradient-Weighted Inversion Line Length (GWILL)

Based on 13 years of MDI line-of-sight data, 71,000 magnetograms, and 6,000 flares, Mason and Hoeksema (2010) found the GWILL to be the most correlated with solar activity. Following from Mason and Hoeksema (2010), the GWILL is computed and generalized for vector magnetogram data. The GWILL is defined below, where L represents single-pixel long segments along the inversion line. The gradient is computed in the six pixels perpendicular to the length.

$$GWILL = \frac{\sum_i (\nabla B)_i \bullet L_i}{\sum_i (\nabla B)_i}$$

An automatic algorithm (Mason and Hoeksema, 2010; Freeland and Handy, 1998) detects the inversion line, shown in red:

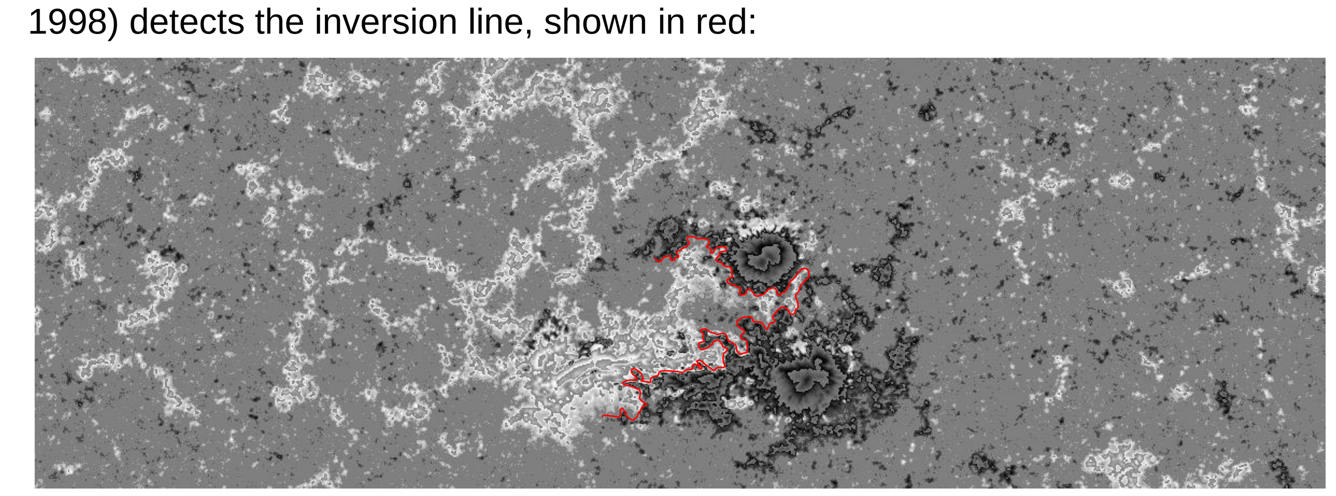

Below is GWILL as a function of time varies little for AR 1117, which produced a C2-class flare on October 25, 2010 at 22:10 UT. There is little variation in the parameter over time, perhaps due to the small size of the associated flare:

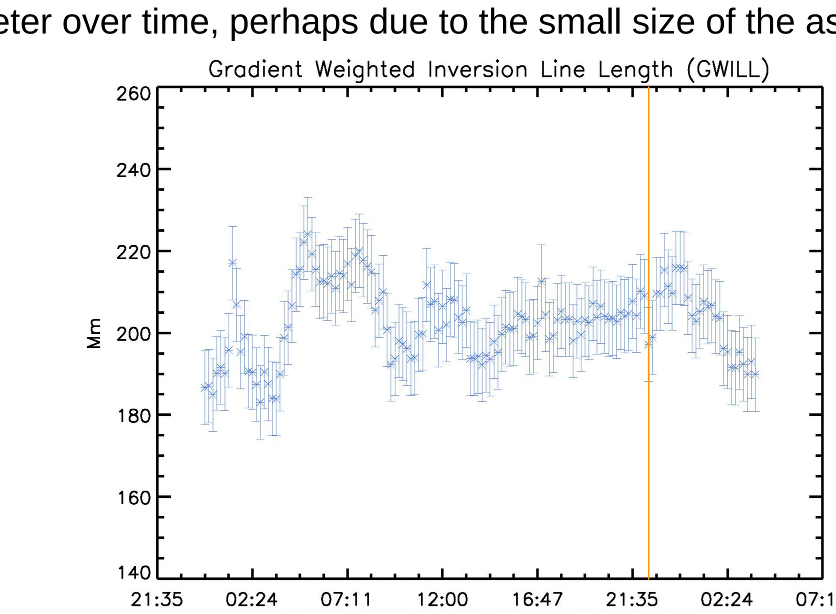

Section 4: Conclusions

Using data from the University of Hawai'I Imaging Vector Magnetograph (IVM) Leka and Barnes (2003) computed spaceweather parameters for 3 active regions. The values presented here agree closely with those of Leka and Barnes (2003), except for the values of alpha and helicity, which are smaller by an order of magnitude. This is likely because HMI has more sensitivity in the horizontal component of the magnetic field, especially in the umbra. Thus we conclude that the HMI vector magnetic data are of high quality, and it is useful to provide spaceweather parameters in near real-time as a regular HMI data product.

Further work needs to be done in particular on the disambiguation process, which may be causing some errors in our result. Further work must also be done on the GWILL parameter, which must be best optimized for a vector field. In addition, stringent conclusions are contingent upon larger sample of active regions.

References

Borrero, 2010, Sol. Phys., 35
Freeland, S.L, & Handy, B.N, 1998, Sol. Phys., 689, 1433
Schou et al., 2010, Sol. Phys., 177
Leka, K.D., et al., 2009, Sol. Phys., 260, 271
Leka, K.D., & Barnes, G., 2003, ApJ, 595, 1296 (Paper II)
Leka, K.D., & Barnes, G., 2003, ApJ, 595, 1277 (Paper I)
Mason, J.P, & Hoeksema, J.T., 2010, ApJ, 723, 634, and references therein
Metcalf, T.R., 1994, Sol. Phys., 155, 235
Scherrer, P.H., et al., Sol. Phys., 162, 129